

Experimental Study on 3-Dimensional Reinforced Concrete Core Wall for Super High Rise Buildings

Tsunehisa MATSUURA

Technical Research Institute, HAZAMA Corp., Japan

Toshio MATSUMOTO

Technical Research Institute, Ando Corp., Japan

Kazushi SHIMAZAKI

Kanagawa University, Japan



SUMMARY:

A structural system using a coupled reinforced concrete (RC) U-shaped core wall, which carries the majority of seismic lateral forces, improves the design flexibility of super-high-rise RC condominium. This experimental study is composed of two test series using the design strength of 60 MPa concrete. The first test is 'lateral loading test' of three 1/10-scale RC core walls, which evaluates the influence of the horizontal loading angle (0, 45, 90 degrees) on the wall capacity design. The second one is 'uni-axial loading test' of extracted core wall elements (i.e. corner, web and edge), which assesses the axial compressive capacity of confined and non-confined concrete. By means of the moment-curvature biaxial analysis with the fiber model, considering the confined concrete characteristics, confined region and the hinge length, it was possible to evaluate the flexural deformation component of the lateral loading test results.

Keywords: reinforced concrete; shear wall; loading test; fiber; modeling

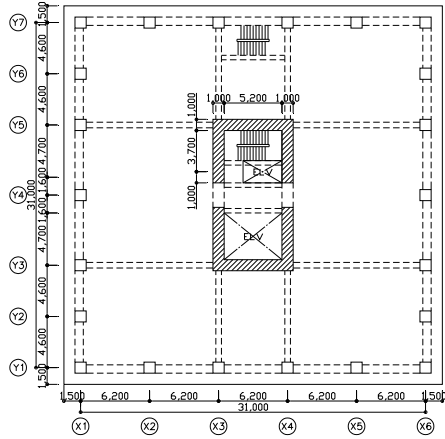
1. INTRODUCTIONS

In the past years, the number of super high rise reinforced concrete (RC) condominium buildings have increased rapidly in Japan. These buildings have been conventionally designed as structural framing systems. However, recently there has been a growing demand for more free space in the inside of the condominium itself, then the design tends to be based on a free plan. In order to create space that can be designed more flexibly, the super-high-rise reinforced concrete condominium building with an earthquake-resistant reinforced concrete U-shaped core wall (core wall below) at the center of the building was proposed.

A structural system using a coupled reinforced concrete core wall, which carries the majority of seismic lateral forces, improves the design flexibility of super-high-rise RC condominium. This study is used to develop the core wall structure applied to super-high-rise RC condominium of 120m in height class.

2. RESEARCH SIGNIFICANCE

During an earthquake, a large axial force acts on the bottom of a core wall that is a multi-story shear wall, in the super-high-rise reinforced concrete condominium building with an earthquake-resistant reinforced concrete core wall. Therefore, the strength and compressive ductility of the core wall under large axial force are important. Especially, a ductility capacity of concrete in the high compression stress area influences the seismic performance for the core wall. In the experimental study on the core wall, many studies intended for L type section are executed. However, the number of the research on C type section wall in the building shown in Figure 1 is a few. This paper describes the two test series and comparisons between experimental results and analytical results.



Building use: condominium
 Structure: reinforced concrete
 Building scale: 31 stories
 Core wall thickness: 1000mm
 Compressive strength of concrete: 60 MPa
 Reinforcement strength: USD685

Figure 1. Building for trial design

3. EXPERIMENTAL PROGRAM

This experimental study is composed of two test series using the design strength of 60 MPa concrete. The first test is 'lateral loading test' of three 1/10-scale RC core walls, which evaluates the influence of the horizontal loading angle (0, 45, 90 degrees) on the wall capacity design. The second one is 'uni-axial loading test' of an extracted core wall element (i.e. corner, web and edge), which assess the axial compressive capacity of confined and non-confined concrete.

3.1. Outline of core wall test

3.1.1. Test specimen information and materials

The specimen was a reinforced concrete earthquake-resistant walls composed of three bottom stories of the core wall of a prototype building (Figure 1). The specimens were shaped like a square without one side. All of the three specimens used in the test were designed to the same specifications. The direction of lateral force was varied from 0 degree to 45 and 90 degrees as a parameter (specimens CW-0, -45 and -90 were made). Figures 2 and 3 show the shape of the specimen and the reinforcement arrangement in the cross section of specimen, respectively. The core wall had a thickness t_w of 100 mm. The transverse wall reinforcement 2-D6@55 (SD345) and vertical wall reinforcement 2-D10@50(USD685) were arranged. Longitudinal reinforcement, 4-D13 (USD685), was arranged in the corners and at the end of the core wall. Concrete in an area of approximately two times the core wall thickness ($2t_w$) was confined using rectangular welded hoops, D6@55 (USD685). Design compressive strength F_c was set at 60 MPa; however, strengths at the time of testing ranged from 64.1 to 66.1 MPa. Table 1 and Table 2 lists the mechanical properties of the materials used in the test.

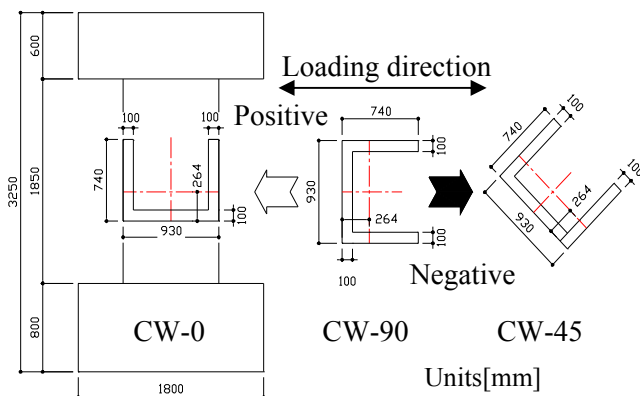


Figure 2. Details of specimen

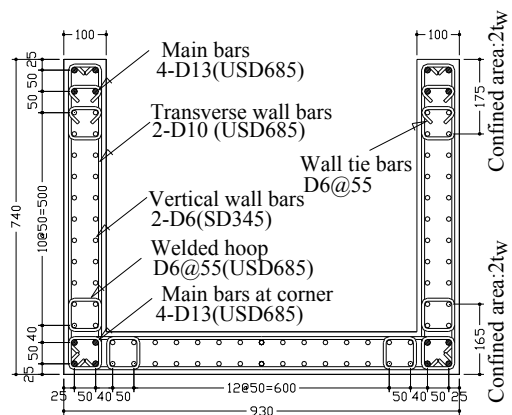


Figure 3. Bar arrangement

Table 1. Mechanical properties of concrete

Specimen	Compressive Strength (MPa)	Yung's modulus (MPa)
CW-0	64.1	35300
CW-45	66.1	34700
CW-90	65.9	33900

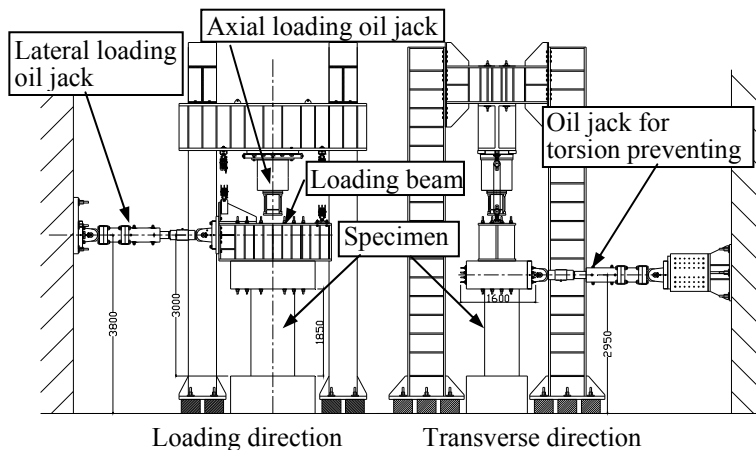
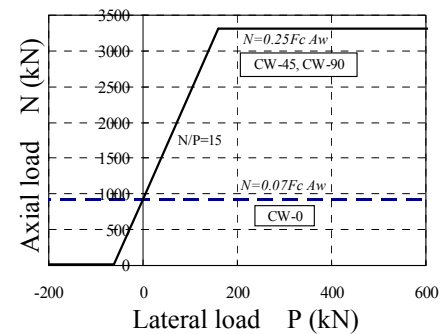
Table 2. Mechanical properties of steel

Using part	Bar diameter	Yield stress (MPa)	Tensile strength (MPa)
Vertical wall reinforcement	D13	745.0	938.0
	D10	729.0	894.0
Transverse wall reinforcement	D6	365.0	524.0
Hoop	D6	699.0	909.0

3.1.2. Loading and measurement methods

Figure 4 shows the loading device. The bottom stub of the specimen was fixed to the test bed and lateral force was applied to the specimen via the loading beam attached to the top stub. The relationship between axial and lateral forces is shown in Figure 5. Specimen CW-0 was applied at $0.07 F_c \cdot A_w$ (A_w : area of core wall full cross section), equivalent to a long-term axial force. For CW-45 and -90, axial force was varied from 0 to $0.24 F_c \cdot A_w$ corresponding to lateral force to simulate the variation of axial force during an earthquake. Both the axial and lateral forces were applied to the centroid of all specimens. For CW-0 and -45, two jacks transverse to the direction of lateral force were used to restrain out-of-plane torsion (Figure 4).

The height at which lateral force was applied was determined so as to simulate the moment gradient on a story in the Y direction identified by seismic response analysis of the prototype building. Lateral loading was applied at a height of 3000 mm from the bottom of the wall. Loading was, however, controlled at a height of 715 mm, equivalent to the height of one story of the specimen. Cyclic loading was applied once where $R (\times 1/1000 \text{ rad.}) = \pm 1.25$, and twice each where $R = \pm 2.5, \pm 5, \pm 10, \pm 15$ and ± 20 . Here, the drift angle of member R is value in which the displacement at a height of 715mm was divided in height 715mm. The horizontal displacements and axial deformations measured at several nodes of the core wall. Strain gauges were placed in the reinforcing bars at major positions for measurement.

**Figure 4.** Test set-up**Figure 5.** Relation with axial load and lateral load

3.1.3. Results of core wall test

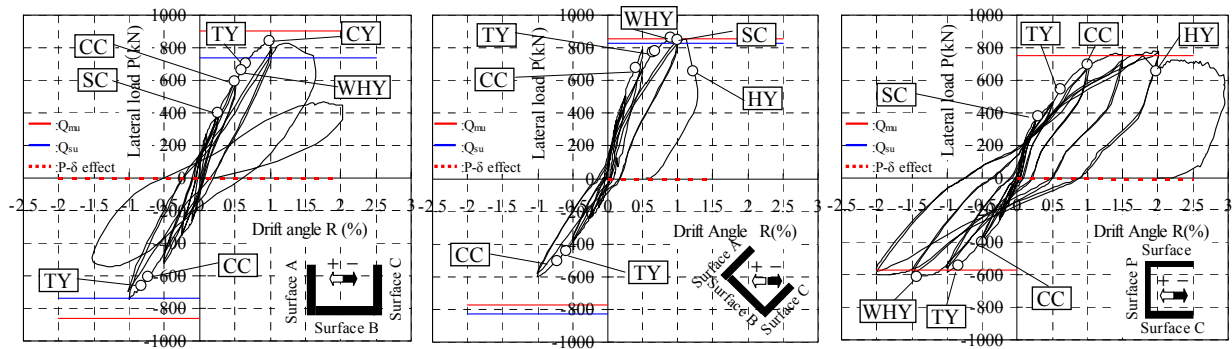
Test results are listed in Table 3. Figure 6 shows the relationship between lateral load P and the drift angle R of the member at the level equivalent to the height of one story. Photograph 1 shows the condition of ultimate failure of each specimen. The observed behavior of each specimen is described below.

In CW-0, shear cracks and crushing of concrete in corners were observed at $R = +2.5/1000$ and $+5/1000$, respectively. The main reinforcement in corners yielded in tension at $R = +6.5/1000$ and in

compression at $R = +9.8/1000$. The maximum lateral force was exhibited at $R = +10/1000$ either during loading or unloading. The spalling of the cover concrete in unconfined sections on surface B of the wall was observed. When R exceeded $+10/1000$, shear failure occurred on surface B of the wall and horizontal load-carrying capacity decreased. Axial load-carrying capacity was maintained, so loading was continued until at $R = +20/1000$. It was determined that CW-0 suffered shear failure after flexural yielding.

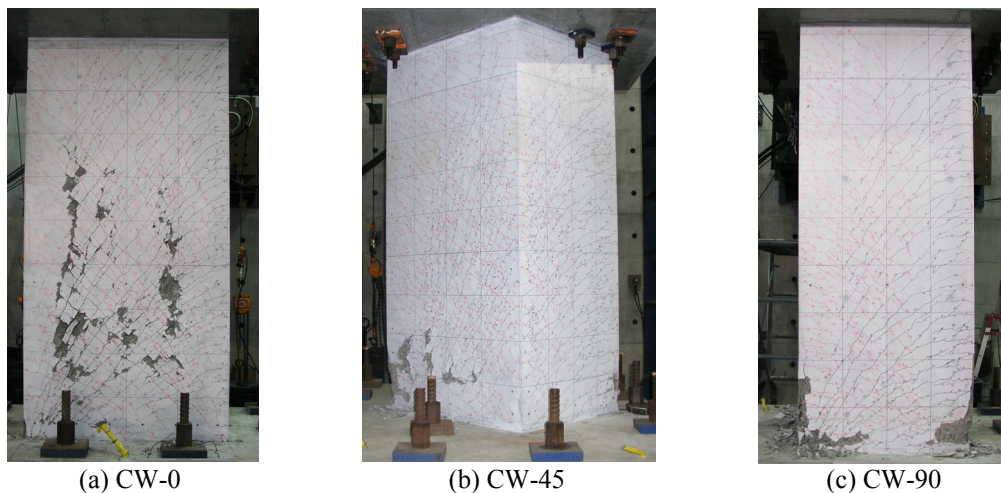
In CW-45, flexural cracks that occurred on surface C of the wall from $R = +1.25/1000$ to $+2.5/1000$ propagated to surface B at $R = +5/1000$. In the negative process, lateral and diagonal cracks occurred on surfaces A and B, respectively, and propagated to surface C at $R = -2.5/1000$. Minor crushing occurred in the corners at the bottom of the wall at $R = +4/1000$. At a drift angle of $R = \pm 10/1000$, the maximum strength was reached. In further loading, the bottom of the wall crushed around the confined area in the corners on surfaces A and B, and vertical reinforcements buckled and load-carrying capacity decreased rapidly. It was determined that CW-45 failed due to flexural compression.

In CW-90, signs of crushing were observed at the end of surfaces A and B of the wall at $R = -2.5/1000$ during unloading. Concrete spalling was found in the corners and at the center of surface B at $R = +10/1000$ during loading. The maximum strength was reached at $R = +20/1000$ but no reduction of strength due to the crushing of wall plate was recognized either during loading or during unloading. Further loading resulted in severe crushing at the bottom of surface B of the wall accompanying the buckling of vertical reinforcements. Axial load-carrying capacity was, however, maintained throughout the test. It was determined that CW-90 also suffered flexural failure.



Notes: SC=shear crack; CC=concrete crush; TY=main bars yielded in tension; CY= main bars yielded in compression; HY=hoop yielded; WHY=transverse wall bars yielded; Q_{mu} =flexural strength; Q_{su} =ultimate shear strength

Figure 6. Lateral load- displacement responses



Photograph 1. Condition of ultimate failure

Flexural and ultimate shear strengths of specimens were calculated based on the material properties shown in Table 1 (Table 3 and Figure 6). Flexural strengths were obtained in cross-sectional flexural analysis (Chapter 4.1). Ultimate shear strengths Q_{su} were obtained using New RC equation (Kabeyasawa and Matsumoto 1992), which is given by

$$Q_u = t_w \cdot l_{wb} \cdot h p_s \cdot \sigma_{sy} \cdot \cot \phi + \tan \theta (1 - \beta) \cdot t_w \cdot l_{wa} \cdot v \sigma_B / 2 \quad (3.1)$$

here

$$\beta = (1 + \cot^2 \phi) p_s \cdot \sigma_{sy} / (v \cdot \sigma_B) \quad (3.2)$$

$$\tan \theta = \left[\sqrt{(h_w / l_{wa})^2 + 1} - h_w / l_{wa} \right] \quad (3.3)$$

$$v = 1.7 \sigma_B^{-1/3} \quad (3.4)$$

$$\cot \phi = 1.5 \quad (3.5)$$

Where t_w is thickness of the wall panel, h_w is height of the wall, l_{wb} is equivalent width of the wall panel in the truss mechanism, l_{wa} is equivalent width of the wall panel in the arch mechanism, σ_B is compressive strength of concrete, σ_{sy} is yield strength of shear reinforcement, and p_s is shear reinforcement ratio within the wall panel.

For CW-45 to which loading was applied at 45 degrees, the angle between the direction of in-plane shear strength of surface B of the wall and the direction of loading was considered based on the mode of failure. When compared with the maximum lateral force during loading, the strength calculated based on the mode of failure was on the safe side for CW-0 and -90. For CW-45, however, there was no difference between flexural and shear strengths. Flexural failure and shear failure may have therefore occurred in combination.

Table 3. Test results

Specimen	Experiment				Calculated	
	Loading direction	Flexural crack load (kN)	Shear crack load (kN)	Maximum load (kN)	Flexural strength Q_{mu} (kN)	Ultimate shear strength Q_{su} (kN)
CW-0	Positive	137	398	856	902	740
	Negative	-75	-310	-753		
CW-45	Positive	302	385	902	853	825
	Negative	-69	-144	-589	-770	
CW-90	Positive	203	377	817	752	1140
	Negative	-58	—	-610	-572	

3.2. Element test for core wall

In order to verify unconfined compression characteristics of concrete used in the cross-sectional flexural analysis of core wall, a test was conducted for the uni-axial loading test of extracted core wall elements (i.e. corner, web and edge).

3.2.1. Specimen and method of test

Table 4 lists the specimens. Figure 7 outlines the element test specimens. Four basic specimens simulated four different areas of the core wall (i.e., corner, web and edge). Additional four specimens were made for loading in areas in compression, and another of a different scale than the others and three for verifying the effect of reinforcement in rectangular cross section were also made. Thus, a total of 12 specimens were made. Measurements were taken over a length equal to approximately two times the wall thickness (100 mm). The reinforcement along the perimeter of the section above and below the length of measurement was at pitches nearly half the spacing of horizontal reinforcement in the length of measurement. The top and bottom ends of the specimen were welded to the vertical reinforcement via 9-mm-thick steel plates.

Concrete was placed the same one as the wall part of the core wall test specimens. Material strength was, however, tested for element test specimens at the time of element test because they were at different ages from the core wall test specimens. The specimens for monotonic loading had compressive strength σ_B of 66.5 MPa and Young's modulus E_C of 36.3 GPa at the age of 63 days. The specimens for cyclic loading had σ_B of 67.0 MPa and E_C of 35.8 GPa at the age of 95 days. The same reinforcement as used in the core wall test were adopted.

Table 4. Details of specimens

Specimen	loading type	cross section (mm)	main bars	hoop	wall tie bar
C-1-M	monotonic loading	100x100	4-D13	D6@55	-
W-1-M		100x190	4-D10 +	D6@55	D6@55
W-2-M		100x200	4-D13	D6@55	2-D6@55
W-3-M			(D6@55)	-	
W-2-55-M			8-D10	D6@55	2-D6@55
W-2-110-M			D6@110	2-D6@110	
W-22-55-M		6-D10	D6@55	1-D6@55	
C-2-M	200x200	16-D13	D6@55	-	
C-1-C	cyclic loading	the same as C-1-M			
W-1-C		the same as W-1-M			
W-2-C		the same as W-2-M			

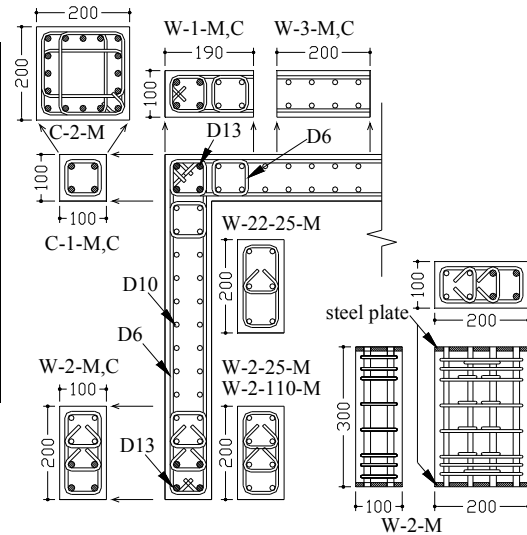


Figure 7. Details of specimens

A 5.0 MN compression tester was used for loading. The rotation at both ends of the specimen was restrained (confined). The specimen with plaster capping on both top and bottom ends was installed on the tester. The hysteresis loop in cyclic loading was defined for C-1-C and W-1-C by simulating the strain history obtained for CW-45 in the core wall test. For W-2-C and W-3-C, the strain history obtained for CW-90 in the core wall test was simulated. Axial loads, displacement at four positions over the length of measurement, and strain of typical vertical and lateral reinforcements were measured.

3.2.2. Test results

Figure 8 shows the relationship between the load bearing capacity of concrete and strain. The load bearing capacity was calculated by subtracting the load bearing capacity of axial reinforcement calculated from the measured strain of reinforcement under a perfect elast-plasticity condition from the total load. Strain was calculated from the displacement in the measurement section as the mean strain in the measurement section.

Figure 8(a) shows the load-strain relationship for W-3-M and W-2-110-M based on measurement, and the load-strain relationship calculated based on the results of concrete material test and using the equation of Fafitis and Shah (1985) based on the assumption that the whole cross section was effective. In both specimens with low specific volume, strength rapidly decreased after the maximum strength, and the calculated strain of lateral reinforcement did not reach the yield strain. The maximum strength of W-2-110-M was approximately 85% of the result of the material test.

Figure 8(b) shows the comparison of the measured and calculated load-strain relationship for W-2-55-M, W-2-110-M and W-22-55-M. The calculation results obtained for the specimens except W-2-110-M using an equation of Sun and Sakino (1993). Two different sectional areas were used for the calculation. One is where full cross section was effective, and other is the core cross section that was defined by the centreline of lateral reinforcement along the perimeter. The equation of Sun and Sakino (1993) nearly represented the area with a descending part in the case of an effective full cross section for W-22-55-M with a few spreaders despite slight over-estimation.

Figure 8(c) shows the comparison of the measured and calculated load-strain relationship for C-1-M and C-2-M, rectangular cross sections of pilasters in the corner. The calculated results could represent the area with a descending part for C-1-M where the core cross section was effective despite under-estimation for C-2-M. This may be because the spalling of cover concrete at a level near the maximum load resulted in subsequent axial displacement not measured accurately.

Figure 8(d) shows the comparison of the measured and calculated load-strain relationship for C-1-M, W-1-M, W-2-M and W-3-M. The calculated results satisfactorily represented the area with a descending part for core cross sections for all the specimens except W-3-M until the strain exceeded 1.5% after the maximum load.

Figure 8(e) shows the relationships between the load carried by concrete and reinforcement, and strain for the specimens subjected to cyclic loading and monotonic loading. The specimens subjected to cyclic loading exhibited slightly greater load carried by concrete and reinforcement than those subjected to monotonic loading near the level of the maximum loading. The relationships between the load carried by concrete and reinforcement, and strain remained nearly unchanged either under cyclic or monotonic loading. In the element test in this study, cyclic loading had a small influence on the shape of an envelope for the descending part.

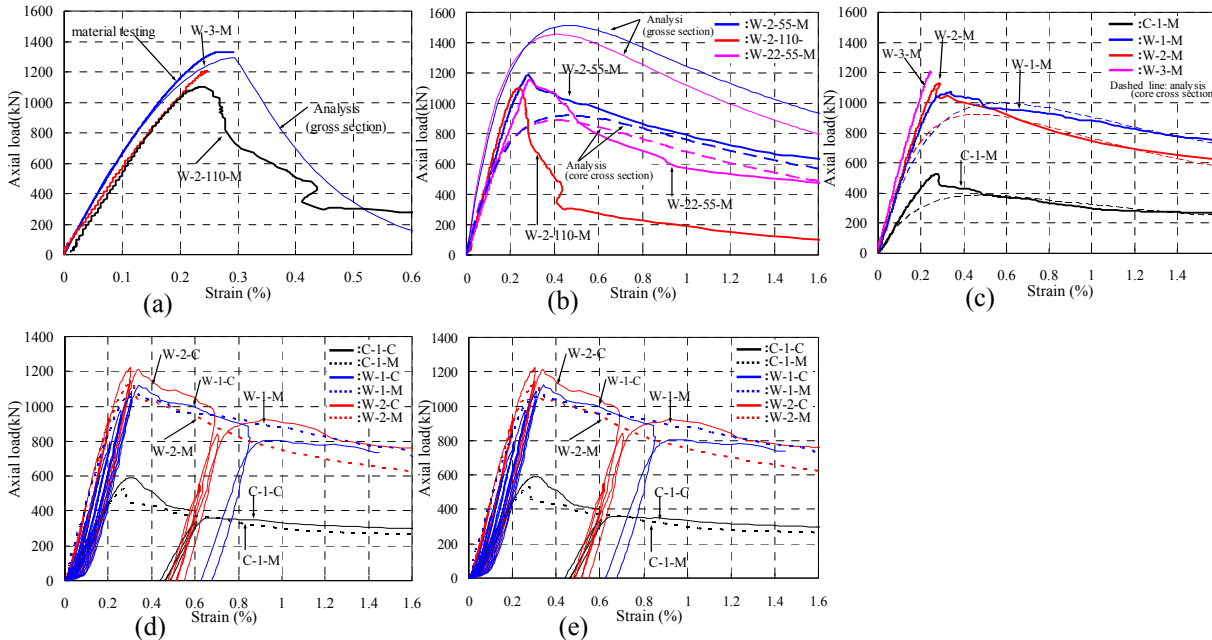


Figure 8. Axial load-axial strain responses

4. ANALYSIS OF CORE WALL

4.1. Sectional analysis by fiber model

Flexural strength was obtained for each specimen in cross-sectional flexural analysis using a fiber element model based on the Navier's hypothesis. The cross section of the analysis model was divided into the section of concrete confined by closed-type hoops and wall tie bars, and the section of plain concrete (Figure 9(a)). Stress-strain curve for the concrete is shown in Figure 9(b). The confined concrete was modelled using the equation of Sun and Sakino (1993) based on the results of the element test. Plain concrete was modelled using the equation of Fafitis and Shah (1985). Reinforcement was represented by a perfect elasto-plastic model.

Test results were compared with analysis results. Figure 10 shows the comparison of the measured and

calculated moment-curvature relationships. Adopted for the curvature of the test result was the mean curvature in a 100-mm measurement section at 75 mm above the bottom that was unlikely to be affected by the separation of reinforcement from concrete. The curvature of the experimental results adopted the average curvature, to reduce influence of pulling out of reinforcement from the concrete. Herein, the average curvature was calculated by the displacement of the measurement section at 75mm from the bottom ends of the wall. The initial stiffness obtained in the analysis was nearly in agreement with the test result. For CW-90, the analytical result well agreed to the test value until large deformation occurred. As for the moment-curvature relationships of the core walls, an estimate is possible by the sectional analysis by the fiber model based on Navier's hypothesis, by evaluating characteristics of concrete adequately.

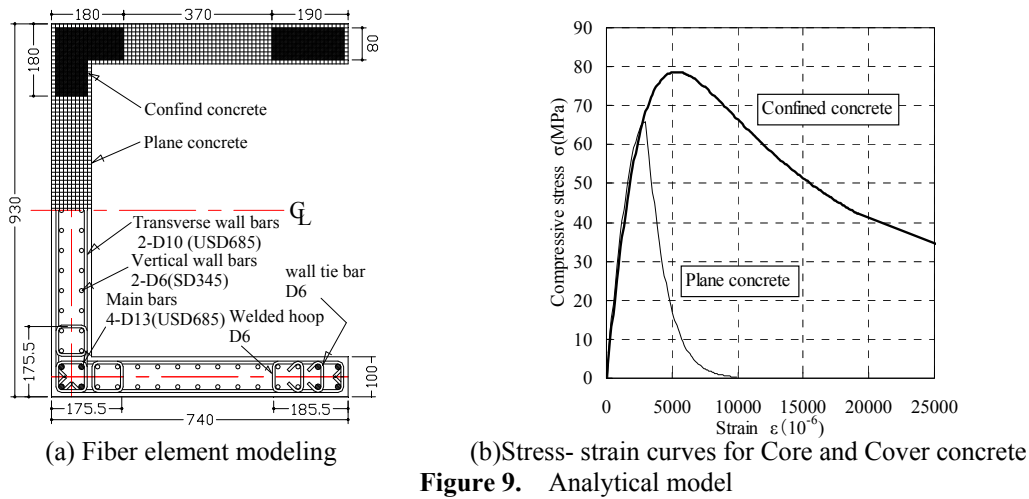


Figure 9. Analytical model

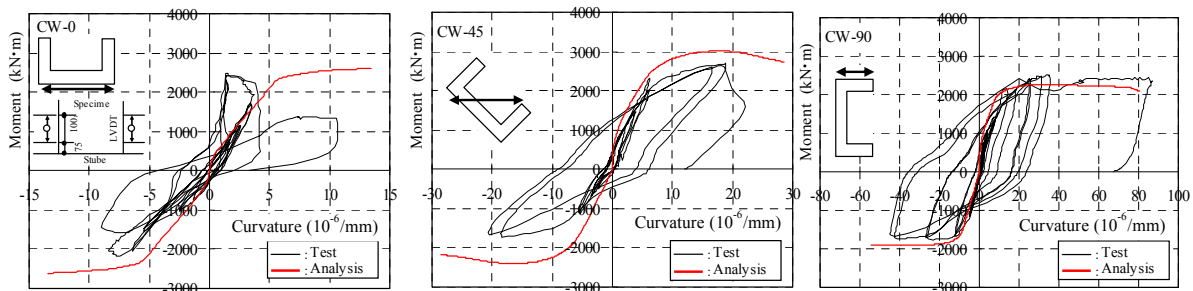


Figure 10. Comparison of experimental and analytical results

4.2. Analysis by three-column model

Here, detailed comparisons are made between the experimental results and the analytic results obtained with the three-column model. Figure 11 shows the three-column model (TIS Inc. 1999), which is a modified model proposed originally by Kabeyasawa et al. (1983) for a multi-story plane shear wall. In making a model of the core wall specimen, the section in the confined area surrounded by main reinforcing bars D13 of the pilaster was regarded as a boundary column and modelled as a truss member. The remaining section was regarded as a wall panel and modelled as a beam. The specimen was divided vertically into three sections and a top stub. When modelling members, flexural strength was obtained from cross-sectional flexural analysis assuming that ultimate flexural strength was developed when the compressive strain of concrete at the extreme fiber was 0.3% or tensile strain of reinforcement was 1%. For calculating the strength against shear crack and the ultimate shear strength, an equation in the Design Guidelines for Earthquake Resistant Reinforced Concrete Buildings Based on Inelastic Displacement Concept (A.I.J 1999) and equation (3.1) were adopted, respectively.

In the analysis, vertical spring was attached at the bottom of the wall in the analysis model to consider

additional deformation due to the pullout of reinforcing bars from concrete. The spring stiffness was calculated from the elongation of reinforcement at the yield longitudinal reinforcement based on the assumption that the reinforcement anchorage length was $40d$ (d : diameter of reinforcing bar) and that strain was distributed linearly in the anchorage area. Here, spring stiffness was calculated in consideration of pullout of reinforcement and, however, without compression of concrete. Lateral load was applied to CW-45 and CW-90 while axial force was varied. Axial force reached the upper limit due to small deformation, in analysis, the axial force used was a constant value at the upper limit. As boundary conditions, displacement transverse to the direction of lateral force applied to the stub was restrained.

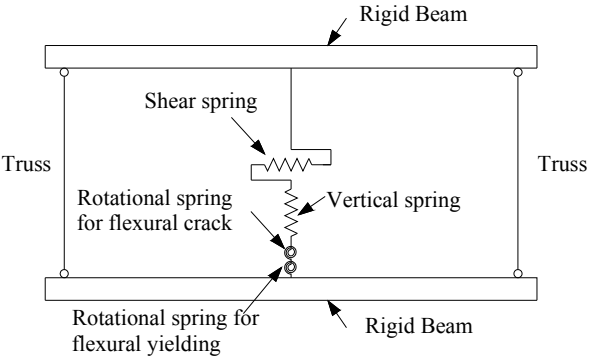
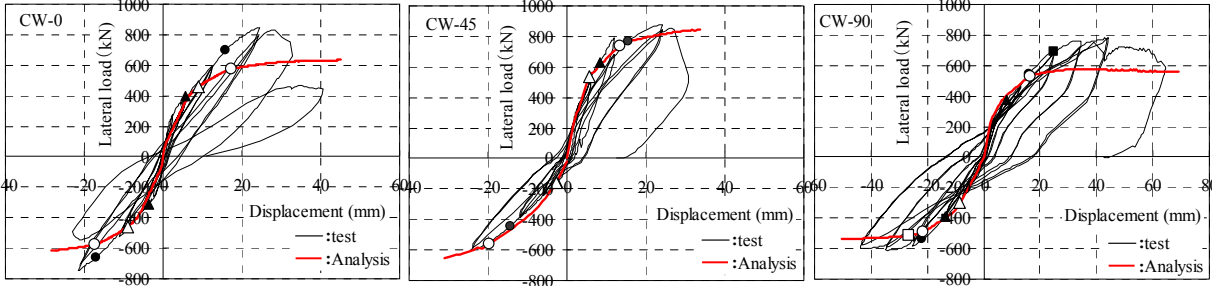


Figure 11. Three-column model

Figure 12 shows the relationship between lateral load and displacement at the position of the top stub. Key events during testing such as appearance shear crack, and main bars yielded in tension or compression are marked on the plots. A good agreement is seen between the analytical initial stiffness and test data for all specimens. In comparison between test results and analysis results, calculated displacement and load carrying capacity at the longitudinal bar yielding were accorded with experimental value. There was, however, as for displacement at the shear cracking, a difference occurs in test results and analysis. The Load carrying capacity in tests exceeds that of analysis value in CW-0 and CW-90. The failure mode was shear failure after flexural yielding in the test and flexural failure in the analysis for CW-0; flexural compressive failure in the test and shear failure after flexural yielding in the analysis for CW-45; and flexural compressive failure in the test and flexural failure in the analysis for CW-90.



Notes: \blacktriangle =shear crack; \bullet =main bars yielded in tension; \blacksquare = main bars yielded in compression; \diamond =shear ultimate strength. The explanatory notes of white paint shows the analytical result.

Figure 12. Lateral load- displacement responses

In the quasi 3-dimensional analysis by the structural design program (TIS Inc. 1999), the result of sectional analysis by the fiber model was used as the flexural strength. The ultimate flexural strength was determined using the strain of concrete or reinforcement as described earlier. As a result, the flexural strength in the quasi 3-dimensional analysis by the structural design program was smaller than the result obtained in 4.1 sectional analysis by the fiber model. In view of this point, the analysis result was in good agreement with the skeleton curve of load-deformation relationship for the test result. Then, the three-column model (TIS Inc. 1999) is applicable to the analysis of core walls without pilaster.

5. CONCLUSIONS

For developing a high-rise reinforced concrete condominium building, a lateral loading tests of a three-dimensional earthquake-resistant wall and uni-axial loading tests of an extracted core wall element. The following conclusions are derived the tests and analyses.

Lateral loads were applied in varying directions to three reinforced concrete three-dimensional earthquake-resistant walls (U-shaped core walls). As a result, the failure mode was shear failure after flexural yielding where lateral load was applied at 0 degrees. The failure mode was flexural compressive failure where lateral load was applied at 90 degrees. In the case of lateral load applied at an angle of 45 degrees, shear failure mode may have been combined with the flexural compressive failure.

Tests were conducted for the uni-axial loading test of extracted core wall elements (i.e. corner, web and edge). As a result, it was found that the equation of Sun and Sakino (1993) could represent the stress-strain relationship of concrete including the effect of cyclic loading for the concrete effective for restraint. In sections where concrete is not expected to produce the effects of restraint, equations for plain concrete including the one of Fafitis and Shah (1985) should be used.

The flexural strength of core wall could be calculated in cross-sectional flexural analysis using a fiber element model based on the Navier's hypothesis by using the equation of Sun and Sakino (1993) for concrete in confined area, and the equation of Fafitis and Shah (1985) for concrete in unrestrained area.

Analysis was made for core walls without any pilasters like those used in the tests in this study using the quasi 3-dimensional analysis by the structural design program based on the three-column model (TIS Inc. 1999). As a result, the three-column model was found to be applicable to core walls.

REFERENCES

- Toshimi Kabeyasawa and Kazuyuki Matsumoto,(1992). Tests and analyses of ultra-high strength reinforced concrete shear walls, *10th World Conference on Earthquake Engineering*, **Vol.IV**:3291-3297
- Fafitis, A. and Shah, S.P.,(1985). Lateral Reinforcement for High-Strength Concrete Columns, *ACI SP-87-12*, 213-232
- Yu Ping Sun and Kenji Sakino,(1993). Ductility Improvement of reinforced Concrete columns with High Strength Materials, *Proceedings of the Japan concrete Institute*, **Vol.15:2**:719-724,(in Japanese)
- TIS Inc.(1999). ADAM/3D-LIMIT Program Manual, TIS Inc., Tokyo,(in Japanese)
- Toshimi Kabeyasawa, Shunsuke Otani and Hiroyuki Aoyama,(1983). Nonlinear dynamic analyses of R/C Wall-Frame Structures, *Proceedings of the Japan concrete Institute*, **Vol.5**:213-216,(in Japanese)
- Architectural Institute of Japan(AIJ),(1999). Design Guidelines for Earthquake Resistant Reinforced Concrete Buildings Based on Inelastic displacement Concept (Draft), Architectural Institute of Japan, Tokyo